Fermilab

Fermi National Accelerator Laboratory
P.O. Box 500 • Batavia, Illinois • 60510

TD - 00 - 069
September 29, 2000

Nb_3Sn Cos(θ) Dipole Magnet, HFDA-01 Production Report

N. Andreev[1], D. R. Chichili[1], I. Terechkine[1], S. Yadav[1], and A. Zlobin[2]
[1]Engineering and Fabrication Department
[2]Development and Test Department
Technical Division
Fermilab, Batavia, IL 60510

1.0 Introduction

HFDA-01 is the first of a series of Nb_3Sn Cosθ dipole models to be fabricated and tested at Fermilab as part of the High Field Magnet Program for a future Very Large Hadron Collider (VLHC). The dipole model is a 1 m long magnet with a 43.5 mm bore aperture. The coil structure and the mechanical support elements are shown in Fig. 1. The model consists of two layer cosθ coil structure made out of Rutherford type cable, aluminum spacers, yoke halves, aluminum clamps, stainless steel skin and end-plates.

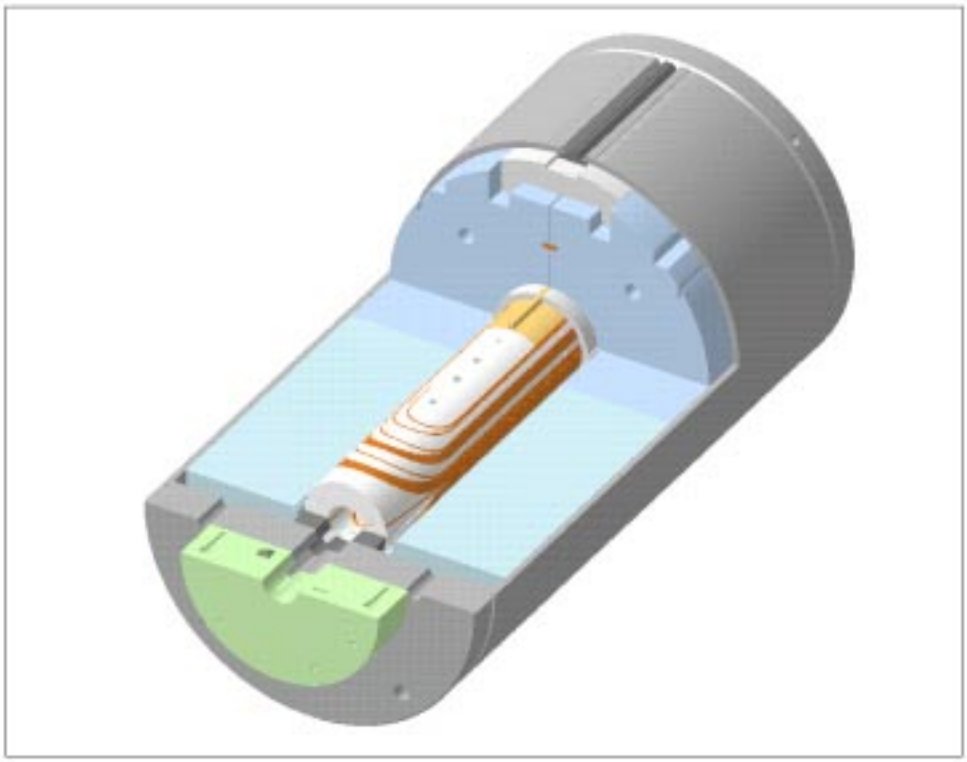

Figure 1: *3D model of the dipole magnet.*

This report presents in detail the fabrication steps and procedures and the data collected during the production dipole model, HFDA-01. The report is divided into the following sections; Strand and Cable, Coil Fabrication, Coil Reaction, Epoxy Impregnation, Instrumentation, and Magnet Assembly.

2.0 Strand and Cable

The conductor used for HFDA-01 was manufactured by OST using a Modified Jelly Roll process. A cross-section of an unreacted (virgin) strand is shown in Fig. 2. Note that the nominal diameter of the strand is 1.00 mm with an effective filament diameter of 115 μm. The Cu to non-Cu ratio is 0.92. The critical current density for a virgin strand was measured to be about 2.0 kA/mm^2 at 12 T, 4.2 K with a RRR of 30. The degradation due to cabling was measured to be less than 10% for a packing factor of 88.8%.

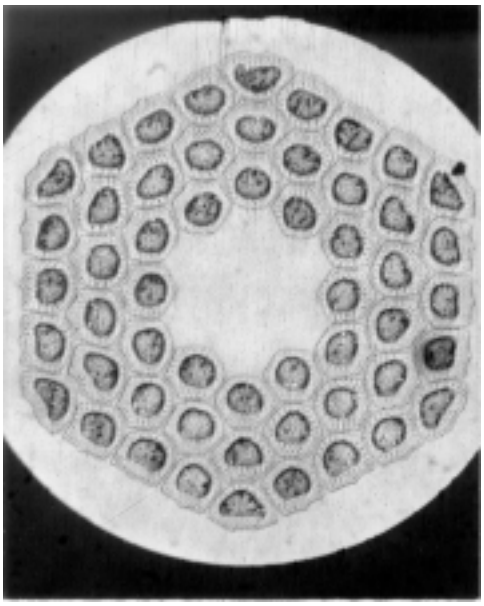

Figure 2: *Cross-section of the unreacted strand.*

PARAMETER	UNIT	DM-1 CABLE
Radial width	mm	14.23
Minor edge	mm	1.707
Major edge	mm	1.933
Midthickness	mm	1.82
Keystone angle	deg	0.927
Pitch Length	mm	109.8
Number of strands		28
Lay direction		Left

Table 1: *Cable parameters as provided by LBNL.*

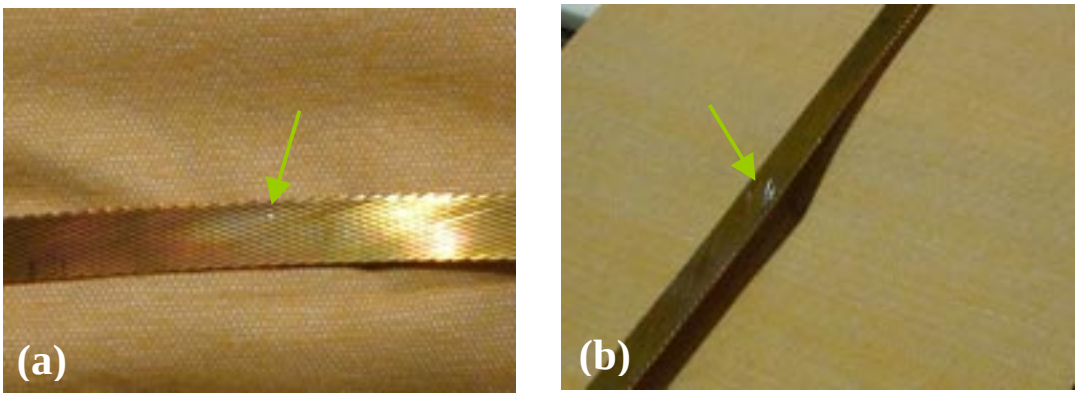

Figure 3: *Stainless steel core (a) stuck between the strands and (b) coming out of the cable*.

Rutherford type cable with a 25 μm thick stainless steel core was manufactured at LBNL. The cable parameters are listed in Table 1. The quality of the received cable was not entirely satisfactory: at several locations we saw the core stuck between the strands (see Fig. 3a). Note that the core did not

come out of the cable surface except at one location, about 131 meters from the start, where the core was sticking out of the cable (see Fig. 3b). The cable was initially cleaned with ABZOL VG to remove any oil left from the cabling process. It was then heat-treated at 200 ^{0}C for 30 min to reduce the residual twist that comes from the cabling process.

3.0 Coil Fabrication

The coil fabrication for the first dipole model started during the first week of April 2000. The first inner coil was discarded after scraping off the conductor while inserting the first return end spacer. Thereafter, corners of the end-parts were rounded to ensure smooth insertion.

3.1 Cable and Wedge Insulation

The cable was wrapped with a 50% overlap ceramic tape using the insulating machine in IB3 (see Fig. 4). The tape held quite well without any breakage during the wrapping process. A thin layer of ceramic matrix (obtained from CTD Technologies) was then applied to the insulated cable using rollers. The entire spool of wet insulated cable was cured at 80 ^{0}C for 20 min. This step was introduced to improve the stiffness of the insulation and hence to reduce any possible insulation breakage, especially while winding around the end parts. Fig. 5 shows the variation of the average thickness of the insulation used on HFDA-01 cable with pressure. Note that the nominal thickness of the insulation is 250 μm. The cured insulated cable was spooled into two reels, an inner cable reel with 64 feet (20 m) plus 15 feet of NbTi leader and an outer cable reel with 85 feet (26 m) plus 15 feet of leader. The leaders were needed for the tensioning device and were soldered onto the Nb_3Sn cable to reduce the total amount of Nb_3Sn cable required per coil.

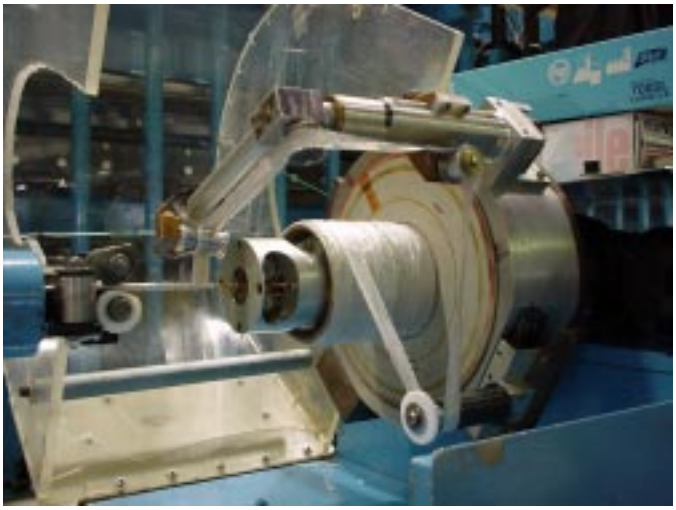

Figure 4: *Insulation wrapping process*

The wedges were insulated by hand according to the assembly drawings MD-376175 and MD-376171 for the inner and outer coils respectively[1]. Ceramic matrix was then applied to the insulated wedges and cured at 80 ^{o}C for 20 min.

[1] Note that as described later in Section 3.6, the insulation on wedges was reduced from 50% overlap butt lap for the second half-coil, to reduce the overall azimuthal coil size.

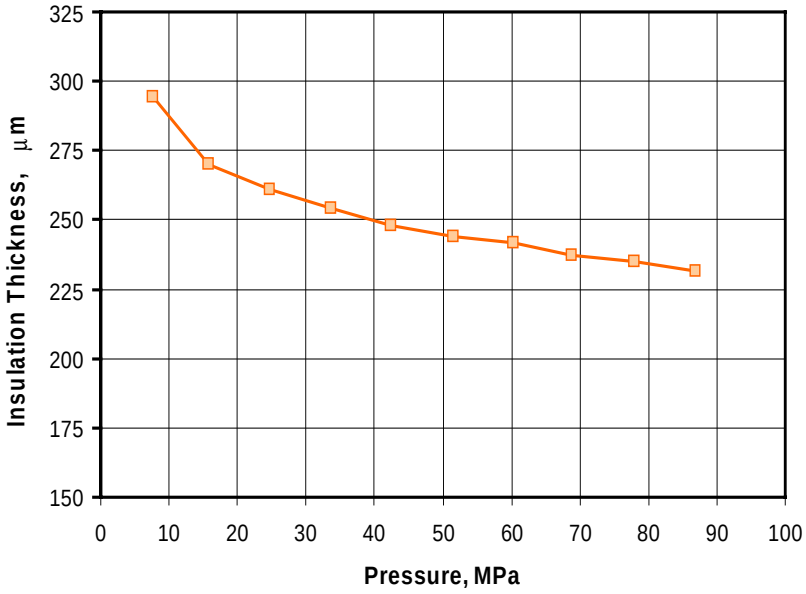

Figure 5: *Variation of insulation thickness with pressure used on DM-1 cable. Note that these measurements were taken after the ceramic binder was applied and cured.*

3.2 Coil End-Parts

The coil end-parts were made out of aluminum-silicon bronze, C642. This material was chosen because of similar thermal contraction coefficient to that of the coil azimuthal direction (3.3 mm/m from 300 to 4.2 K for C642 and 3.5 mm/m for the coil) and because its melting temperature is high enough to withstand reaction temperature. Table 2 lists the chemical composition of C642.

Cu	Al	Si	Fe	Ni
91.2	6.3-7.6	1.5-2.2	0.3 (max)	0.25 (max)

Table 2: *Chemical composition of the C642 aluminum-silicon bronze.*

End parts were designed using program BEND and fabricated at LBNL using a 5-axis wire EDM machine (see the assembly drawings, MD-376175 for inner layer and MD-376171 for outer layer). After fabrication, all parts were sand blasted before applying a 4 mil thick ceramic layer using plasma spray coating. This is to prevent any possible coil to ground shorts.

One of the unique features of the design was the modification of the inner and outer layer lead end shoes to bring the cable out at 15 degrees angle to the midplane, rather than at midplane (see Fig. 6). This was achieved using program LEAD and was performed to provide enough space for the cable splice boxes at the ends. Another unique feature of the design is the absence of any inter-layer splices. A straight ramp transition was machined in the inner and outer layer lead end pole pieces at an angle of 6.42 degrees to the horizontal. The cable transition from the inner to the outer layer was performed over a length of 5.291" (134.4 mm), which is greater than the cable pitch length of 109.8 mm.

Figure 6: (a) *Modified inner layer lead end shoe and (b) outer layer shoe*

3.3 Inner Coil Winding and Curing

The inner coil spool was loaded on the tensioning device and the outer coil spool was hung over the winding table using a crane. A tension of 60 lbs. was applied during the coil winding. A slight tapping of the conductors with a hammer was performed around the end parts to position the conductors in their right position. Fig. 7 shows a wound inner coil with close-ups of the lead end (LE) and return end (RE). Notice the quality of insulation; we did not have insulation breakage during the coil winding. Gaps were introduced in the pole to account for the differential thermal expansion between the pole piece and the cable in the longitudinal direction, during reaction. Voltage taps were installed during the coil winding process. A thin strip of stainless steel was inserted between the cable and the insulation, during winding around the end-parts for the first half coil. For the second half coil, voltage taps made of brass were used. There are three voltage taps on the inner coil RE and four on the inner coil LE per half coil as shown in the Figs. 7(b) and 7(c).

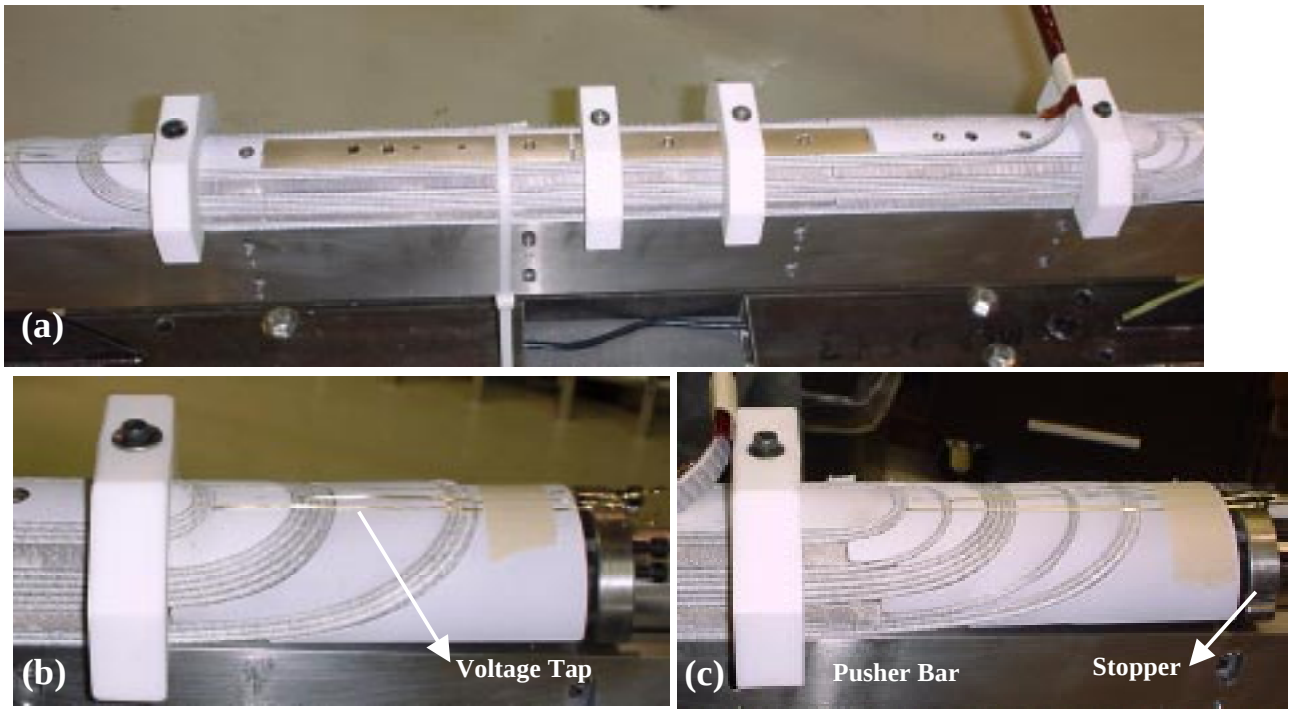

Figure 7: *First inner coil after winding (a) overall coil (b) RE (c) LE.*

After coil winding, the ceramic matrix was applied along the length of the coil using a brush. Since the matrix has low viscosity it quickly spreads to all parts of the coil. The wet coil was packaged for curing by mounting pusher bars on the sides and then placing a retainer over top of the coil. The High Gradient Quadrupole (HGQ) inner coil curing fixture was used for curing the coil. The curing cycle involved initial massaging of the coil at low pressures to seat the coil in place. A final azimuthal pressure of 45 MPa was applied as the insulation thickness reaches the nominal design size at this pressure. A radial pressure of about 10 MPa was applied to obtain the required radial coil geometry. The curing temperature of 150 ^{0}C was held for 30 min. The curing process was designed to be a displacement controlled (mold cavity size) rather than pressure controlled. However we had about 3 to 9 mils of gap at the beginning of the curing cycle and with the increase of temperature the mold cavity closed at all places along the length of the cavity. Finally unlike LHC IR Quads, we had no end pressure. The ends were merely restricted from outward motion through stoppers placed at both ends of the coil (see Figs. 7b and 7c).

Fig. 8 shows the cured inner coil. The quality of the coil was very good with excellent rigidity. The cable to end-part adhesion was slightly weaker than that of turn-to-turn bonding. None of the voltage taps were damaged during the curing process. Detailed mechanical length measurements were taken on the cured coil. Table 3 lists some of the length measurements taken. It is clear from these measurements that the ends are longer than the nominal size.

Figure 8: *Cured Inner coil*.

Parameter	First Inner Coil Inches	Second Inner Coil Inches	Nominal Length Inches
Coil Length	39.700	39.660	39.370
LE Length	13.939	13.868	13.732
RE Length	8.394	8.457	8.299

Table 3: *Inner Coil length measurements taken after curing*.

3.4 Interlayer Insulation

The next step in the production of the half coil was to fabricate and install an interlayer insulation with strip heaters. Tooling was developed to help form the ceramic cloth into shape (see Fig. 9). There were three layers of insulation, each 5 mils thick. The middle layer contained two bands of 1 mil thick stainless steel strip heaters arranged as shown in the Fig. 10(a). The three layers were assembled together on the tooling and then held in place by the side bars. The center cylinder was

then pushed from underneath to remove any wrinkles in the layers. Thereafter, the CTD binder was applied and the whole system was cured at 150 °C for 30 min. The final product is shown in Fig. 10(b). The interlayer insulation was placed on top of the inner coil.

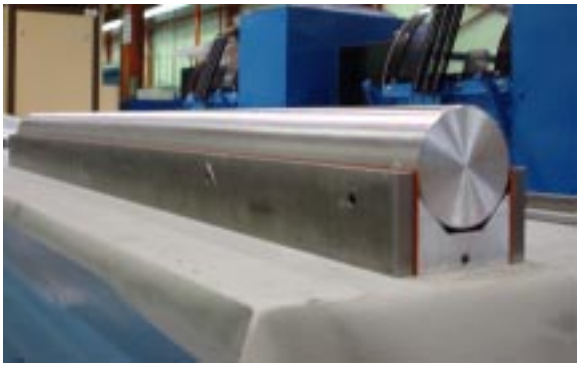

Figure 9: *Tooling for making the interlayer insulation with strip heaters.*

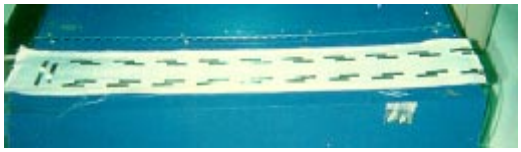

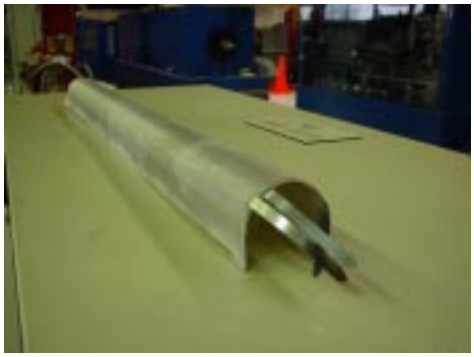

Figure 10: (a) *The middle layer with stainless steel strip heaters, (b) final product*

3.5 Outer Coil Winding and Curing

The outer layer was wound on top of the cured inner coil after the installation of the interlayer insulation. Note that we use a single cable to wind both the inner and outer layers of a half coil, thus requiring no interlayer splicing. The spool designated as the outer layer reel with 85 feet of cable along with 15 feet of leader is now mounted on the tensioner. This spool hangs on top of the winding table during the inner coil winding. The winding of outer coils went smoothly without any technical problems.

The curing of the outer coil was done along with the previously cured inner coil. Fig. 11 shows the cured outer coil. The quality of the coil is quite good. The mold cavity however, did not close completely during the curing cycle. Inspite of increasing the azimuthal curing pressure from 45 MPa to about 60 MPa there was still a gap of 15 to 19 mils between the mold cavity and the upper platen in the center of the mold. We went ahead and cured the coil with this gap. The idea was to remove a layer of ground insulation to compensate for this increase in coil azimuthal size. Length measurements were taken on the cured coil while on the mandrel. Table 4 shows the data. Similar to the inner coil, the overall length of the outer coil is more than the nominal length. This is primarily due to the increase in lengths of the lead and return ends.

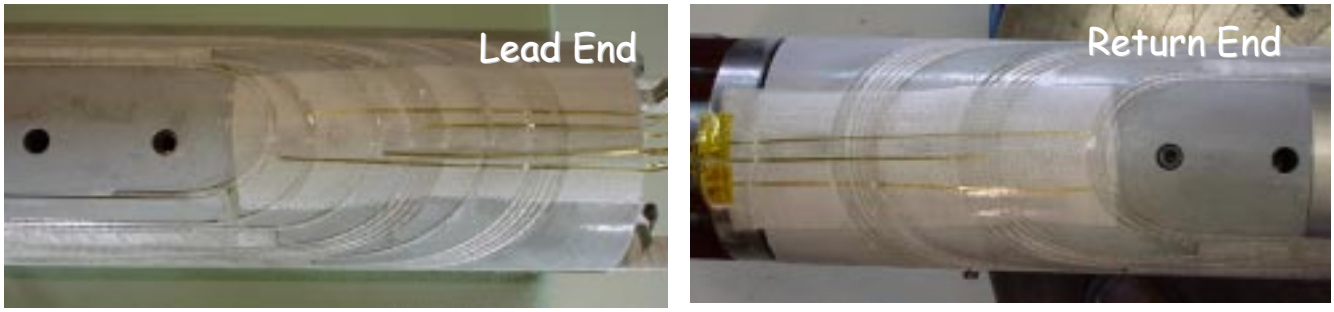

Figure 11: *Cured outer coil with close-up views of LE and RE.*

Parameter	First Outer Coil Inches	Second Outer Coil Inches	Nominal Length Inches
Coil length	39.700	39.840	39.370
LE Length	13.714	13.757	13.535
RE Length	8.455	8.540	8.299

Table 4: *Outer coil length measurements taken after curing.*

3.6 Half-Coil Mechanical and Electrical Measurements

The azimuthal size of the two cured half coils was measured at four positions along the length at varying pressures. Figure 12 shows the data with respect to the nominal size. The dashed lines represent the first half coil and the solid lines represent the second half coil. The mean azimuthal size at a pressure of 2.5 MPa for the first half coil is 0.2 mm and that of second half coil is 0.01 mm over the nominal size. The standard deviation is about 0.07 mm. The insulation overlap of the wedges for the second half coil was reduced from 50% overlap to butt lap to reduce the overall coil size, since we anticipate further increase in size after reaction. The modulus of elasticity in the azimuthal direction for the cured coil was computed from the Fig. 12 and is about 20 GPa. Note that this value was obtained from the linear regime of the curve. The variation in size between Side A and Side B of the first half half coil at Position 3 is shown in Fig. 13. Note that there is a difference of about 250 μm between the two sides. However for practice coil, HFM-PC-03 we had a difference of less than 90 μm.

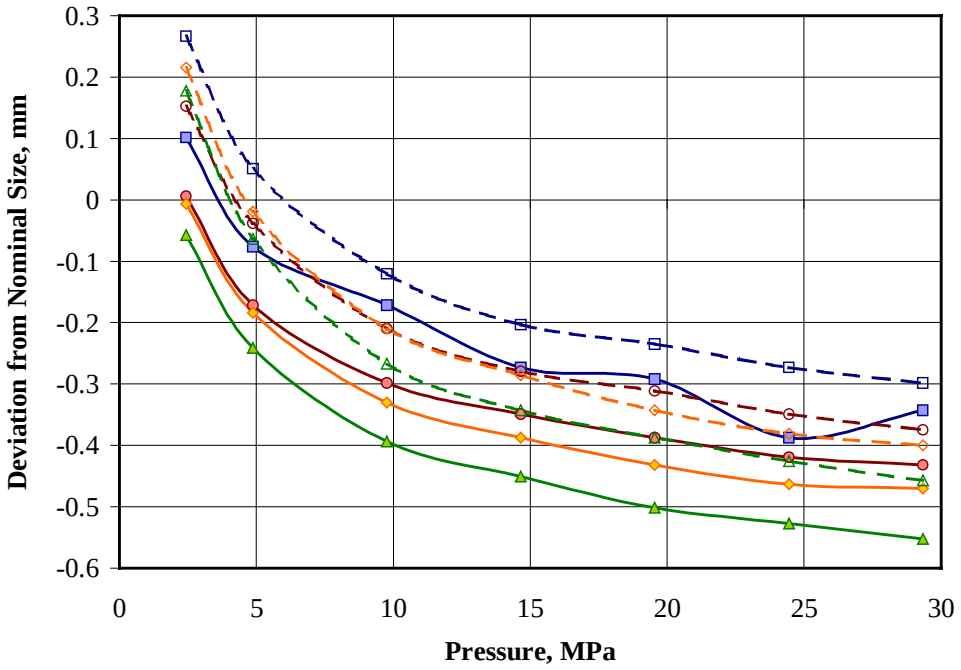

Figure 12: *Azimuthal coil size variation with pressure at four positions along the length of the coil. The dotted lines are for the first half coil and the solid lines are for the second half coil.*

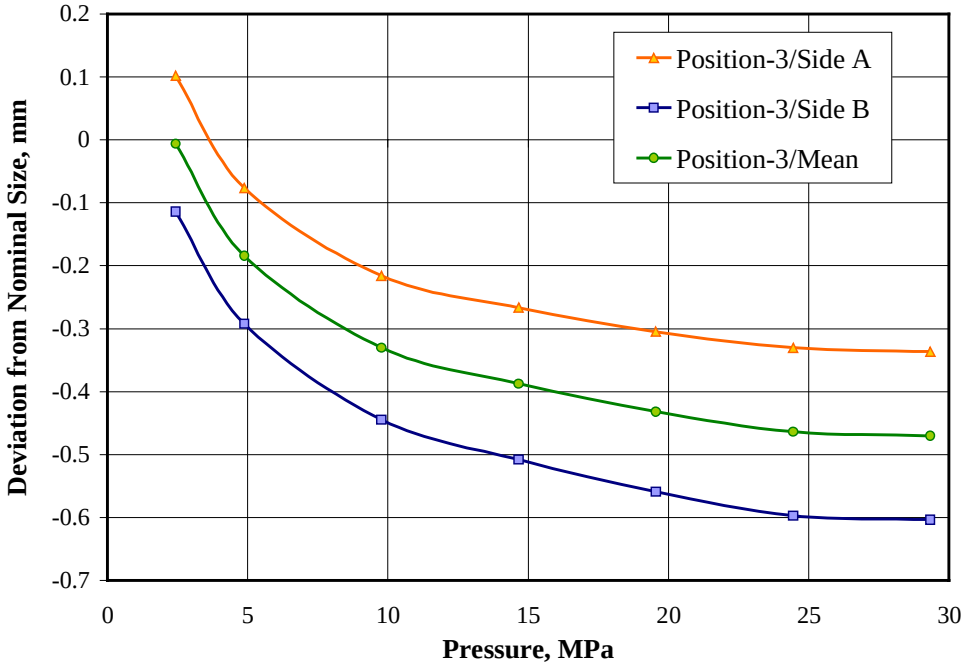

Figure 13: *Variation in size with pressure for Side A and Side B at Position 3.*

Turn-to-turn resistance measurements using a four wire technique at a current of 0.1 mA were performed to check for shorts. Note that these measurements were taken on coils in their free state. Fig. 14 shows the data which suggests that there are no turn-to-turn shorts.

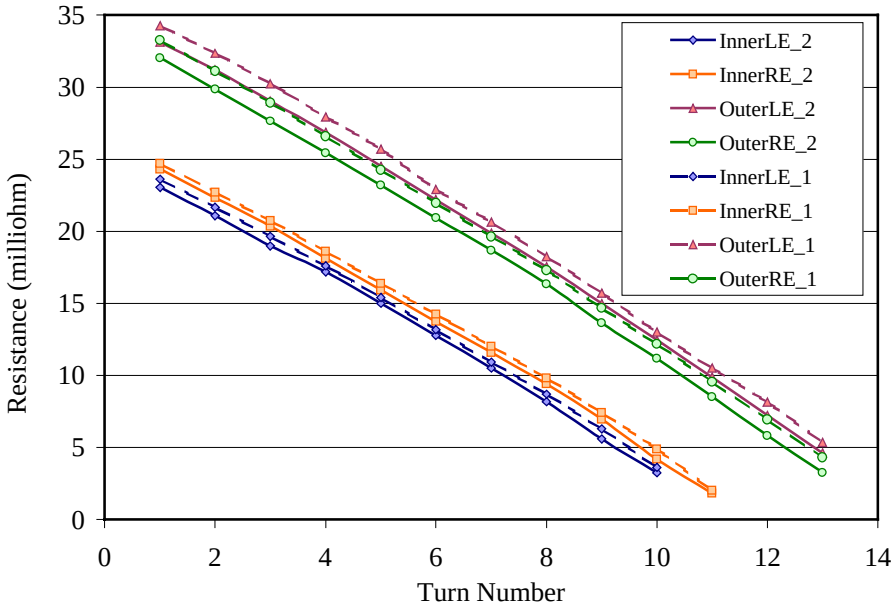

Figure 14: *Turn-to-turn resistance measurements on the two half-coils.*

4.0 Coil Reaction

Ground insulation consisting of three layers of 5 mil thick ceramic cloth was placed on the two half coils. Fig. 15 shows an exploded view of the ground insulation scheme. The three layers of ceramic cloth were preformed into shape using the matrix and a forming fixture similar to that used for interlayer insulation. Since the thickness of the insulation increased with binder, only two layers of ground insulation were added for this magnet.

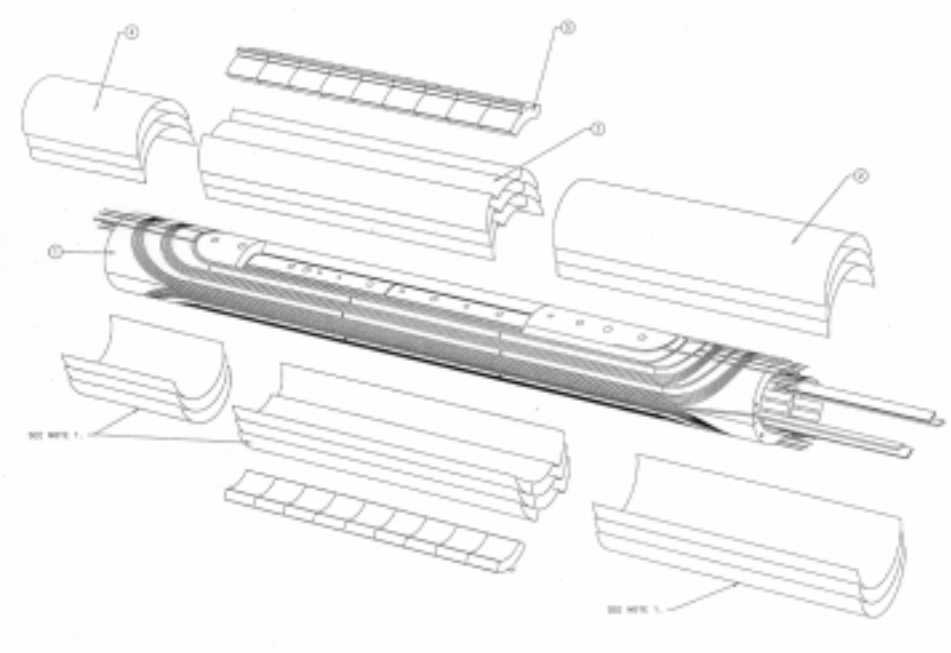

Figure 15: *Exploded view of the coil assembly with ground insulation*; *1-Coil sub-assembly, 2-LE ground insulation, 3-Straight-section ground insulation, 4-RE ground insulation, 5-Pole pieces.*

Fig. 16 (a) shows the coils ready to be placed in the reaction fixture. Before assembling the coils in the reaction fixture, the stainless steel core from the cable leads was removed. This was achieved by tinning the end of the cable, removing the cable insulation, and then unwinding the cable to expose the stainless steel core upto 1" from the lead end. The core was then cut and the cable was rewound. The two half coils were assembled around a stainless steel mandrel (wrapped with a layer of mica tape) and placed into the reaction fixture. Fig. 16 (b) shows the reaction fixture with the coil assembly inside. Since the coil radial size was more than the nominal, an additional pressure of about 8,000 pump psi (equivalent to a force of 4 x 10^5 N) had to be applied while tightening the bolts on the reaction mold. Even with this pressure we finally ended up with a maximum gap of about 5 mils in the center of the fixture. The coil splice supports were then installed to support the cable leads. The leads were cut upto the coil splice support and welded to prevent tin from leaking out during the reaction cycle. The reaction fixture was then placed in a vacuum retort. The whole system was first checked for any possible leaks before placing it in the furnace. The retort was then pumped several hours for vacuum and later purged with Argon gas. The flow rate of Argon was adjusted to 1 cm^3/sec. The reaction cycle used for HFDA-01 is shown in Fig. 17. This thermal cycle was chosen as it gave the best critical current and magnetization properties based on short sample studies.

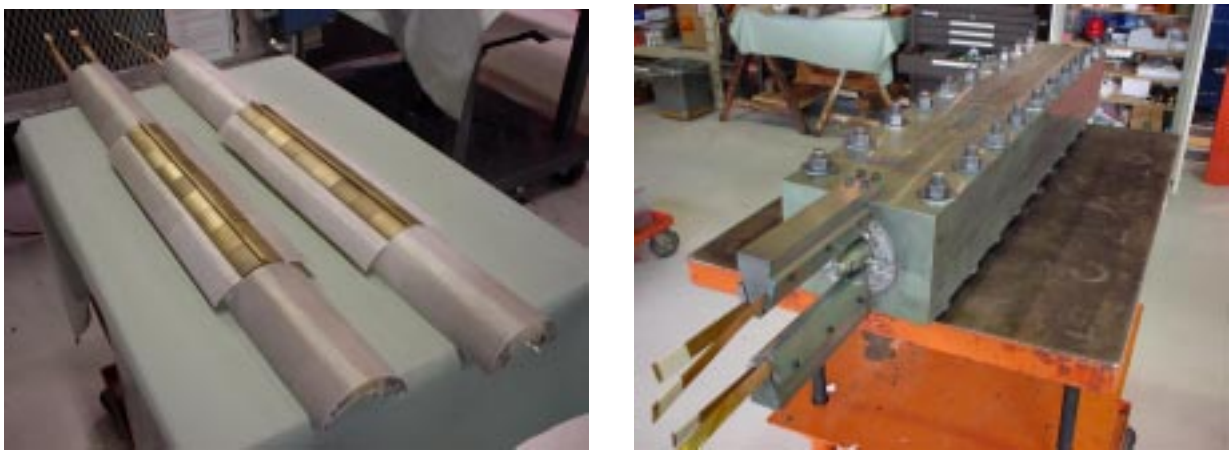

Figure 16: (a) *Two half coils with ground insulation, (b) Reaction fixture with coil assembly*

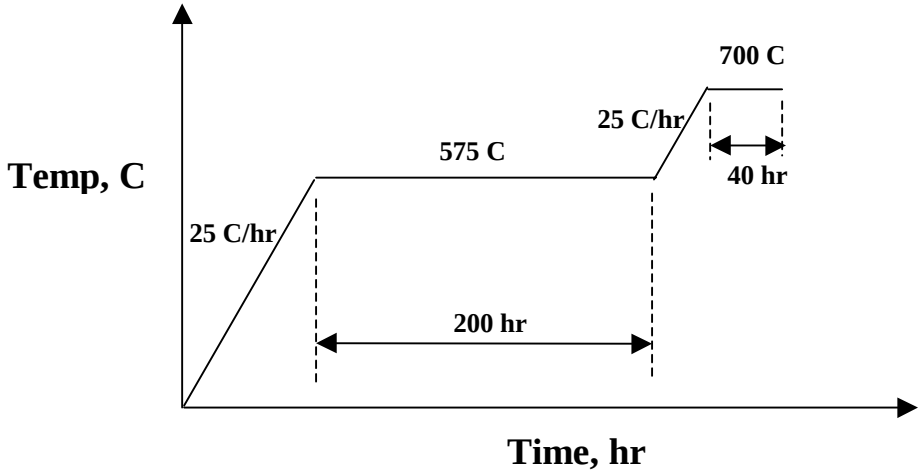

Figure 17: *Reaction cycle used for this magnet.*

After the reaction, the gaps between the two halves of the reaction fixture were measured and the variation of the gap along the length of the fixture before and after reaction is shown in Fig. 18. The maximum gap increased from 5 mils to 15 mils. This increase in gap was to be expected due to increase in the cable width after reaction.

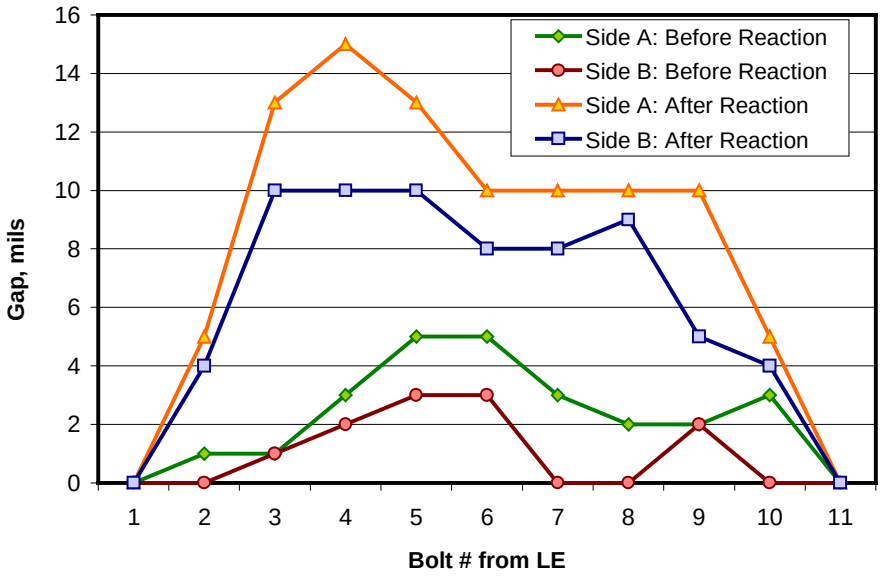

Figure 18: *Variation of gap in the reaction fixture along the length.*

We also observed tin leakage in the leads when we removed the splice supports. The strands were slightly damaged while removing the supports due to sticking of tin to the lead support structure. Fig. 19 shows the damaged area of the HFMI-002 lead. This tin leakage is attributed to the removal of low temperature (200 ^{o}C) step from the reaction cycle where the tin diffuses in solid phase as well as high compaction of coils before reaction. To test the quality of the reaction process, we had also placed some short-sample barrels in the retort to measure the strand critical parameters. We noticed that the short samples taken out of the retort had I_c values 30% less than those measured from the samples reacted in the tube furnace for the same reaction cycle.

Figure 19: *LE view of the dipole model. Note the damaged area due to tin leakage and*

4.1 Post Reaction Assembly

Post reaction assembly involves terminating all the voltage taps and strip heaters both on LE and RE. Care should be taken such that we should be able to access these wires after impregnation. First to prevent any shorts G-10 plates were screwed to the end-spacers on both LE and RE . Slots were provided in the G-10 plates for the wires to be routed. Fig. 20 shows RE view. The white spots on the G-10 plates are slots with voltage tap leads filled with RTV. The idea is to remove this RTV after impregnation to access the leads. On LE, wires were connected to the voltage taps and the strip-heaters and were routed through the slots in the G-10 plate (see Fig. 19) A brass ring with slots was installed next to the G-10 piece after the splice joints were made to secure all these wires during the impregnation. A picture (Fig. 21 (b)) depicting this is shown along with the splice joints in the next section.

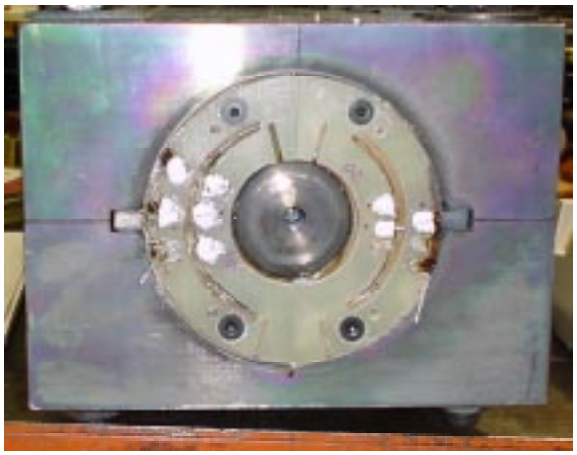

Figure 20: *RE view of the Dipole model with G-10 piece.*

5.0 Splice Joints

The next step in the coil assembly after reaction is to perform Nb_3Sn to NbTi splice joints for the lead cables. The splice assembly consists of a 0.55 mm thick, 125 mm long copper cage, two NbTi cables, one Nb_3Sn lead cable and a 0.55 mm thick, 125 mm long copper top plate. The NbTi splice cable (see drawing # MB-376461) was designed to ensure that two NbTi cables along with the Nb_3Sn cable in the middle results in a rectangular cross-section. Note that a 10 mil thick solder strip was placed between each layer of the cable. The entire geometry was compressed using the splice tooling which is attached to the reaction fixture as shown in Fig. 21(a). Note that two splice joints were done at a time. To support the leads after the splice tooling was removed, a stress relief supporting block was attached to the sides of the reaction fixture (also shown in Fig. 21). The splice joints were made by heating the cables using the heaters provided in the slots of the tooling. The bolts on the tooling were tightened with the increase in temperature until we obtain the right geometry. Fig. 21(b) shows the finished splice joints along with the brass ring and the lead supporting block.

After the coils were assembled into the reaction fixture, the lead cables were not at the nominal position and hence the splice tooling had to be modified to accommodate this. The copper box did not close completely for two of the splice joints. This later created leaks during pumping down for

epoxy impregnation. For future magnets we need to ensure that during coil assembly into the reaction fixture the cable leads are at the nominal position. We will section these splice joints to study the quality of solder joints.

Figure 21: *(a) The cables, copper box and the top plate inside the splice tooling, (b) Finished splice joints with brass ring for voltage tap and heater wires*

6.0 Epoxy Impregnation

6.1 Coil Assembly For Impregnation

The first step is to transfer the coil from the reaction fixture to the impregnation fixture. This transfer should be performed with care so that the conductor is not damaged. A roll-over fixture was designed for this purpose. First the top half of the reaction fixture was removed (see Fig. 22). Some insulation damage was noticed at the pole regions. All the brass voltage taps on HFMO-002 were broken; but the stainless steel voltage taps on HFMO-001 were in a reasonably good condition. This could be a result of applying high pressure to close the reaction fixture and the fact that brass becomes very soft at high temperatures. Relative motion between the coil and the fixture due to differential thermal expansion during reaction might also have caused some damage.

Figure 22: *Reacted coil after removing the top part of the reaction fixture*.

The assembly (coil and bottom half of the reaction fixture) was placed in the bottom half of the roll-over fixture. A 10 mm thick spacer was then placed on top of the coil assembly so that the two halves of the coil separate when we roll over to facilitate the installation of the final layer of mold released Kapton insulation (of 5 mils thickness) in the parting plane. The bottom half of the impregnation mold was then placed on top of the coil assembly and the 10 mm thick spacer. Then the top half of the roll-over fixture was installed and secured. The whole assembly was rolled 180^0 so that the impregnation half goes to the bottom and the reaction half comes on the top (see Fig. 23(a)). The reaction fixture was then removed and a layer of 5 mil thick mold released Kapton insulation was installed. Fig. 23(b) shows the assembly with Kapton insulation installed between the two half coils and around them. At the same time the stainless steel mandrel was removed and a Teflon mandrel was installed. The Teflon mandrel has a clearance of 0.5 mm with the inner diameter of the coils. However the thermal expansion coefficient of Teflon is more than that of the coil, and the clearance is designed such that while curing, the Teflon mandrel expands to fill the whole aperture. On cool down we would still be able to remove the mandrel easily. Practice Coil #2 impregnation showed us that the Teflon mandrel could be removed without significant difficulties. However, if this method fails, the two half coils could also be separated after impregnation as the epoxy does not stick to the mold released Kapton. The process was repeated for the second side to install the Kapton insulation. Splice stress relief fixture which was attached to the reaction fixture has now been reattached to the impregnation fixture.

Figure 23: (a) *Roll-over fixture assembly with impregnation fixture on the bottom and the reaction fixture on the top*, (b) *Coil assembly in the roll-over fixture with mold released Kapton insulation.*

During the process of coil assembly for impregnation we noticed that the length of the coil was larger than that of the impregnation mold. This can be seen in Fig. 23(b). The end of the brass ring should be inside the impregnation mold. After winding and curing, the length of the coils were longer than the nominal size by about 8.4 mm; however after reaction they were longer by about 17.6 mm. This shows that the length of the coil grew by about 9.2 mm during reaction. LBNL and BNL reported that the coil contracts longitudinally after reaction. This is due to release of stored energy in the cable and not due to the formation of Nb_3Sn. In our case we heat-treated the cable at 200 ^oC for 30 min. before winding, during which time the stored energy in the cable would have been released. Note that this step was added into the coil fabrication to reduce the residual twist. So we should not expect contraction in the coil length during reaction. The observed increase in coil

length could be due to the high radial compaction of coil in the reaction fixture. To compensate for the increase in coil length, the length of the brass ring was reduced.

Outer pole extensions were installed in the coil ends before fixing the other half of the impregnation mold. The last step before impregnation process could start was to seal the ends of the mold. The end-plates were designed with slots for the leads to go through and O-rings for vacuum seal. Fig. 24 shows the fixture with coil assembly ready for impregnation. Due to mis-alignment of the coil leads, the O-rings were not effective. We noticed lot of leaks in this area during the leak-check. RTV was applied along the length of the copper box to prevent these leaks.

Figure 24: *Coil assembly ready for impregnation*.

6.2 Impregnation Process

The impregnation process involves the following steps:

1. Perform the leak check on the impregnation assembly.

2. Use the vacuum tank carriage outside the tank to mount the impregnation mold onto the rocking platform MD-376656 so that the middle plane of the mold is vertical. Install the restriction weldment MB-376667 and using crane, lift one end of the rocking platform to install removable weldment MC-376655.

3. Place the support stand with the coil impregnation mold inside the vacuum tank of the Impregnation Facility in IB2 and make hydraulic connections inside the tank in accordance with the scheme in the Fig. 25 below. Be sure that the inlet pipe does not have any vertical loops and waves, but goes smoothly in vertical plane rising from the starting point to the mold. With closed V1, open V2 and V3. Pump out the tank and keep the mold inside the tank for about 24 hours for degassing. Bring the mold temperature to about 60°C in the end of the degassing procedure. Use thermal sensors attached to the mold to adjust the temperature.

4. Epoxy System: CTD 101K
   Make the epoxy mix in accordance with the table below:

Material	Designation	Parts by weight
Resin	Part A	10 Kg
Hardener	Part B	9 Kg
Accelerator	Part C	150 g

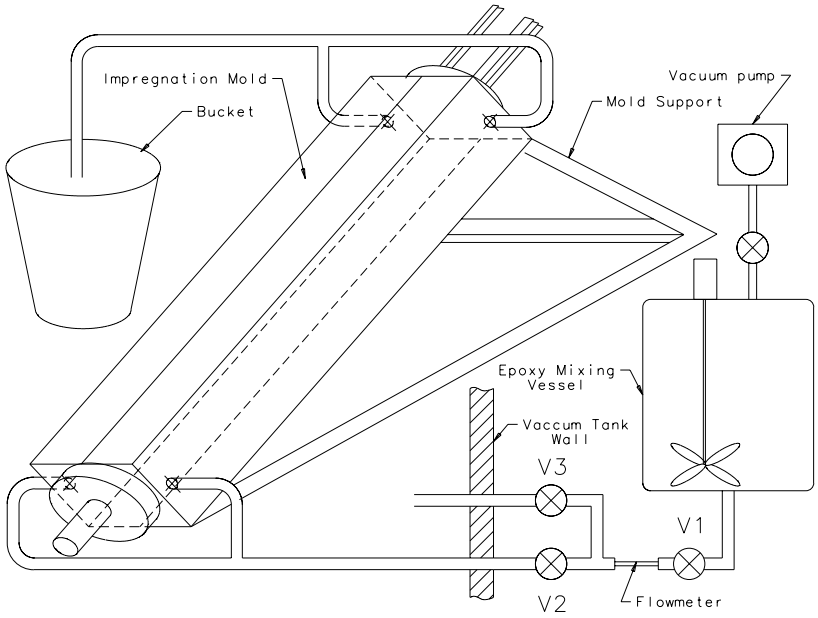

Figure 25: *Schematic of epoxy impregnation set up.*

5. Mixing and degassing Procedure: Combine the weighted components into a container equipped with heating and mechanical stirring. Keep the epoxy temperature of about 60°C during mixing. Use sheet heaters to wrap the container and control the temperature using the controller installed on the Binder Application Machine. Heat and stir the mixture until a clear solution at 60°C is obtained. Degas the mixture at 30 - 40 μm Hg for approximately 40 minutes until the bubbles evolve infrequently from the mixture. The system is now ready for application.

6. Epoxy Impregnation: Connect the hose coming from the epoxy tank (do not release the hose clamp or the tank valve yet) to the valve V1. Open V1 and wait some time until air is removed from the space between V1 and the epoxy tank hose clamp. Close V1, release the clamp, and start the process by slowly opening the valve V1 and letting some epoxy flow trough the flow meter and then close the valve. Inner diameter of the flow meter is chosen to have epoxy flow of about 10 ml/min is its velocity in the pipe is about 0.8 inch/sec Repeat the process until the inlet pipes are filled with epoxy. Watch closely for the epoxy flow using "flow meter". Repeatedly slightly open and close for several minutes the valve V1 allowing about 10-20 ml of epoxy in the mold each time (this corresponds to 1-2 minutes of open V1 state with epoxy flow velocity of about 0.8 inch/sec). Continue the procedure until epoxy is seen in the outlet pipe of the mold. Let epoxy fill the outlet hoses at the top end to account for the contraction during curing. Close valves V1, V2, and apply clamp to the epoxy tank outlet hose. Degas the whole system for about half an hour, then allow air in the

tank, and keep heated mold in the tank for about another half an hour under normal air pressure.

7. Open the vacuum tank, clamp inlet and output hoses, and disconnect the inlet hose from the tank manifold. Remove the tank carriage from the tank, and using crane to lift one end of the mold support, remove the weldment MC 376655. Place the remaining part of the support horizontally, and take the mold to the curing furnace. Be sure that there are no leaks of epoxy.

8. Cure epoxy in accordance with the curing cycle, 5 hrs. at 110°C followed by 16 hrs. at 125 °C. For this magnet the cure cycle was changed to 125 °C for 20 hr.

The impregnation went smoothly and took about 5 hr. to complete. We had problems with the hoses as they were not rated for 125 °C curing temperature. On the exit end copper piping was brazed to have extra epoxy during curing. However in the inlet side we connected the hoses to 4 inch long copper pipes sticking out of the fixture. The impregnation set up as taken after the process as shown in the Fig. 26.

Figure 26: *Impregnation fixture set-up taken after the process.*

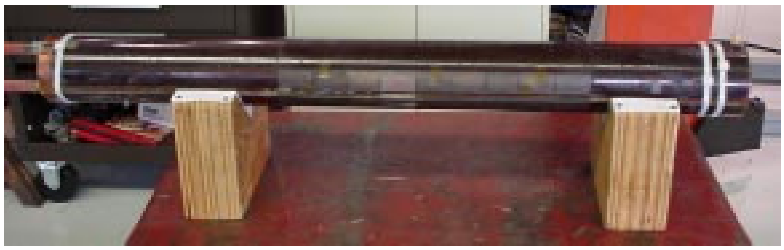

Figure 27: *Impregnated coil structure.*

Due to oversizing of the coil, the impregnation mold did not close completely. The maximum gap between the two halves of the fixture before and after the impregnation was around 0.125 mm. After curing, the coil was carefully removed from the tooling. The Teflon mandrel came out easily. Fig. 27 shows the impregnated coil. The quality of impregnation was quite good. We

noticed some wrinkles in the Kapton layer which might have developed during compression of two halves of the impregnation fixture. The diameter of the impregnated coil "pipe" structure was measured at several locations along the length (Fig. 28). At the mid-pane the coils are about 250 μm more than the nominal size and at the pole region about 75 μm. These measurements were taken in a free state and hence the measurements would be an over estimate.

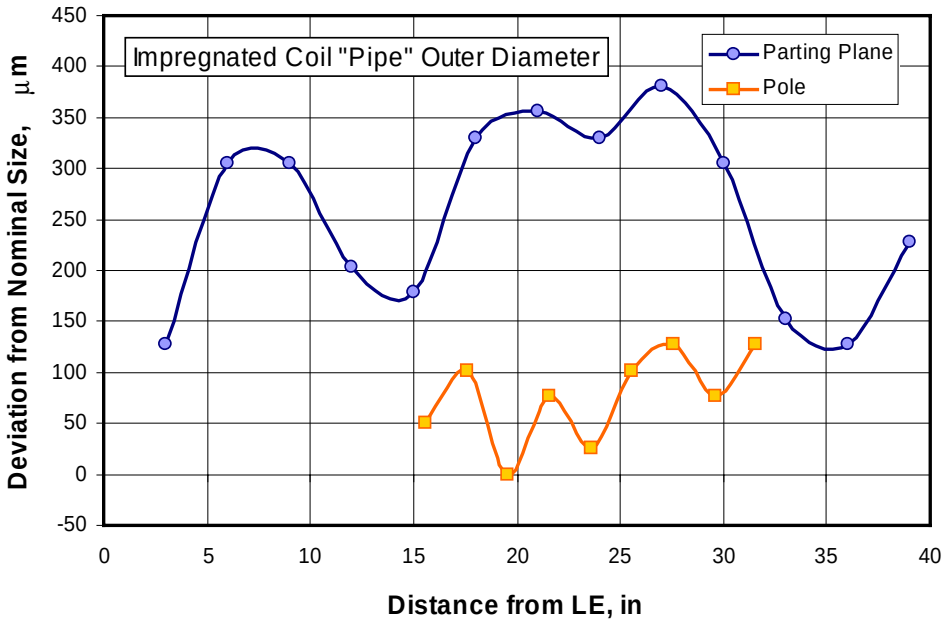

Figure 28: *Impregnated coil "pipe" diameter measurements.*

6.3 Electrical Measurements

The overall resistance, inductance and quality factor for both the half coils were measured after impregnation. The data is given in Table 5. Also given in the table are the values before reaction. Before reaction the two half coils have similar values and match the theoretical estimates. This indicates that before reaction the coils were free of turn-to-turn shorts. However after reaction, the first half coil has low inductance than the second half coil indicating that it has developed shorts. Notice that the resistance of the coils increase with reaction. Turn-to-turn resistance measurements were made on the first half coil by removing the epoxy on top on the conductor to locate the positions of shorts. Figs. 29 and 30 shows the data. In Fig. 29, each data point represents the increment in resistance of half turn starting from outer-most half turn. Therefore for a coil free of shorts we should expect a smooth drop in the resistance. In Fig. 30, each data point represent the increment in resistance per turn starting with the inner most turn. It is clear from these graphs that we have shorts between the turns 9 and 10 near LE and between 6 and 7 near RE in inner layer and between turns 2 and 3 near LE, 5 and 6 in the straight section, and 12 and 13 near RE in outer layer.

When we separated the two half coils we noticed lot of tin leakage in both the half coils. We checked in the inner layer if tin leakage is causing the shorts. Firstly not all the spots with tin leakage are grounded. We identified about 5 areas with tin leakage which had coil to ground short. One of them is between turns 9 and 10 and we tried to repair this spot with no success. The amount

of tin leaked covered the entire width of the cable. At this point we decided not to go ahead with this magnet fabrication. However we wanted to assemble the coils with yoke pieces and put them under press to understand the mechanics.

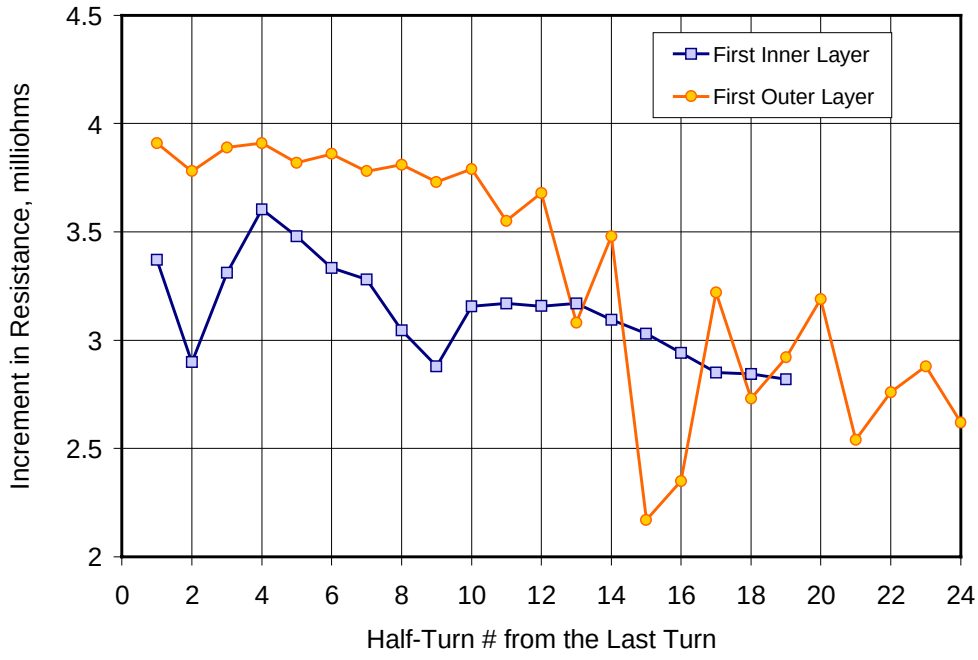

Figure 29: *Increment in resistance of half turn for both inner and outer layers of first half coil.*

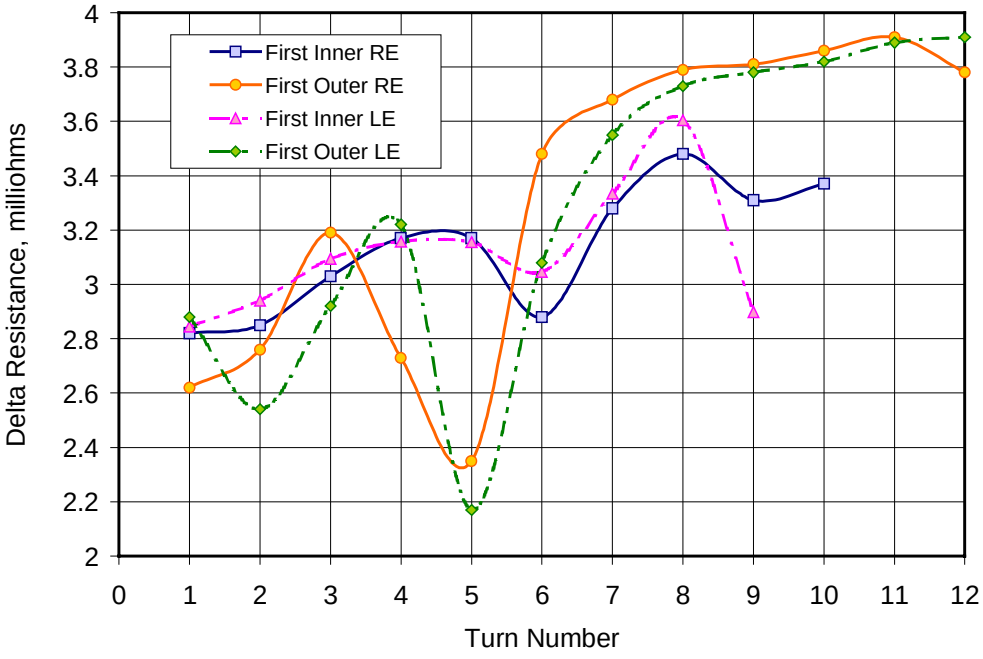

Figure 30: *Increment in resistance per turn for both inner and outer layers in first half coil.*

Parameter	Before Reaction		After Reaction	
	First Coil	Second Coil	First Coil	Second Coil
Inductance, μH	232.4	236.4	94.3	200.8
Quality Factor	6.01	6.36	0.93	2.68
Resistance, mΩ	56.5	62.8	78.6	81.9

Table 5: *Electrical measurements on half-coils*

7.0 Instrumentation

The magnet was instrumented with capacitance gauges and resistive gauges to measure stresses in various components. Fig. 31 shows the layout of the gauges in the magnet cross-section. The four capacitance gauges are used to measure the azimuthal stress in the coils while the four resistive gauges are for measuring the azimuthal stress in the spacers. Circumferential grooves were made on the spacer to install the gauges, where as the arc length of the outer pole pieces were reduced by 20 mils on each side to accommodate capacitance gauges. Note that no attempt was made to measure inner coil stress directly. However resistive gauges were installed on the inner pole pieces to estimate the azimuthal stress in the inner coils.

Capacitance gauges were fabricated and calibrated both at 300 K and at 4.2 K in house. The behavior of these gauges was quite linear and repeatable. Epoxy impregnated ten-stack with ground insulation was used on one side of the capacitance gauge during calibration to simulate the exact conditions in the real magnet. For resistive gauges, the zero readings at 300 K and at 4.2 K were recorded to evaluate the absolute stress in the components after cool down.

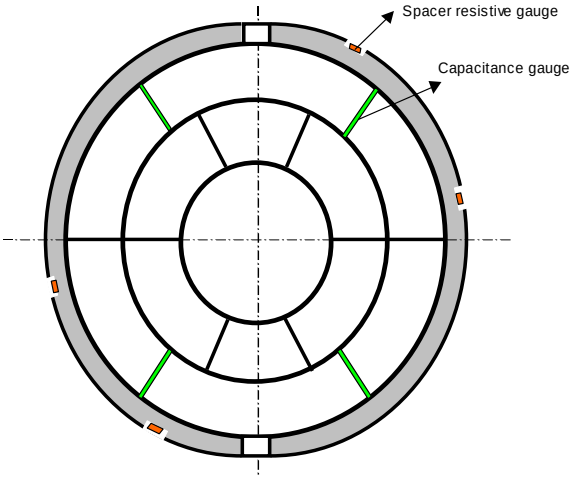

Figure 31: *Layout of gauges in the magnet cross-section.*

8.0 Magnet Assembly

Aluminum spacers were first installed around the two half coils. The whole assembly was then placed into the lower yoke packs. Note that the lower yoke packs are stacked in the bottom half of the contact tooling. The second half of the yoke packs were then installed on top of the coil/spacer

assembly. The second half of the contact tooling is then placed on top of the yoke assembly. Fig. 32 shows the yoked assembly ready to be compressed. Dial indicator were placed between the two platens of the contact tooling to measure the displacement during compression. The pump pressure was increased incrementally and the corresponding displacements were noted. Fig. 33 shows the data for first two cycles. For Cycle-1, the initial displacement is big since the impregnated coil structure was initially in a relaxed state. The displacements thereafter are small. After unloading the dial indicators showed a displacement of about 0.05 inches for Cycle-1 and almost zero for Cycle-2. Further the slope of the line for Cycle-2 is smaller than that for Cycle-1 indicating an increase in coil assembly stiffness.

Figure 32: *Yoke Assembly*.

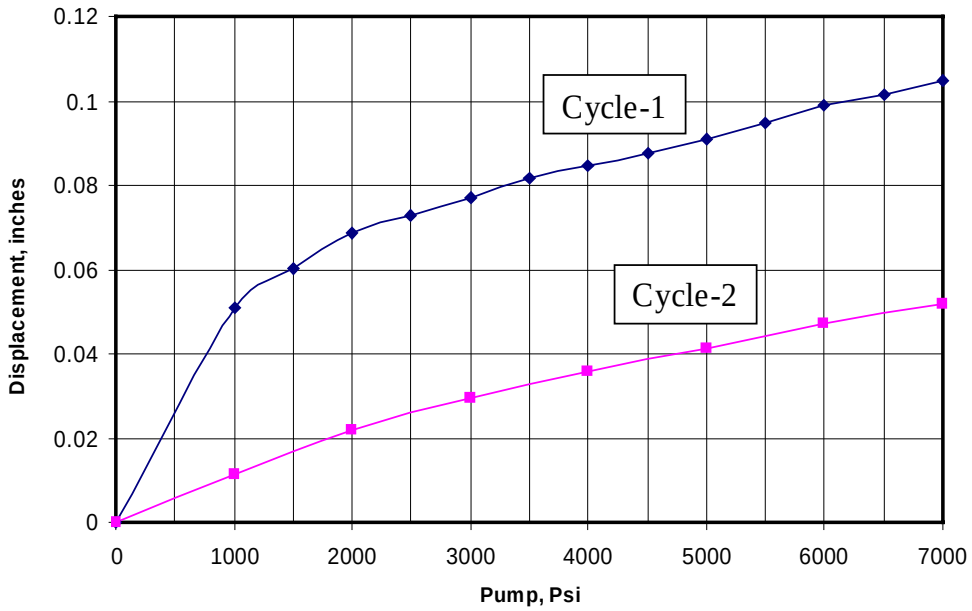

Figure 33: *Displacement of the top platen with pump pressure*.

At the peak pressure of 7000 Pump psi, which is equivalent to 8945 N/mm of force, the gap between the two iron yoke halves was measured to be 1.35 mm in the center and 0.9 mm in the ends. The nominal gap should be 0.9 mm at which point the aluminum clamps could be inserted without much pressure. This measured difference in the gap between the center and the ends is due to bending of the contact tooling. We added a graded shim between the contact tooling and the yoke with a maximum of 30 mils in the center of the magnet. This gave us a uniform displacement of the yoke halves along the length of the magnet. We also changed two cylinders from 100 T to 150 T capacity in the press. At a pump pressure of 9000 psi, which is equivalent to 13000 N/mm of force we achieved almost uniform gap of about 1.0 mm along the length of the magnet.

The capacitance and resistance gauge data were also recorded during this process. Note that the capacitance gauge data provides the azimuthal stress in the outer layer pole region. Two sets of resistive gauges were used to obtain the azimuthal stress in the aluminum spacers at the pole and at the parting plane (PP) region. Note that during initial cycling, the capacitance gauge did not record any change in the capacitance. After disassembly we realized that there is a clearance of about 2 mils between the gauge and the outer pole piece. A 2 mil Kapton layer was installed between the pole and the gauge and the magnet was reassembled. One of the capacitance gauge broke during the assembly. Fig. 34 shows the cap gauge and resistive gauge data during the assembly process. At the peak pressure, the azimuthal stress in the coil near outer pole region is about 100 MPa. The azimuthal stress in the spacer near the pole region is about 200 MPa and 100 MPa near the parting plane. Note that the coil stress in this model is less than in Mechanical Model - 2; whereas the spacer stress is more than that in Mechanical Model - 2. This is because the coil size in Mechanical Model - 2 is larger than in Dipole Model - 1.

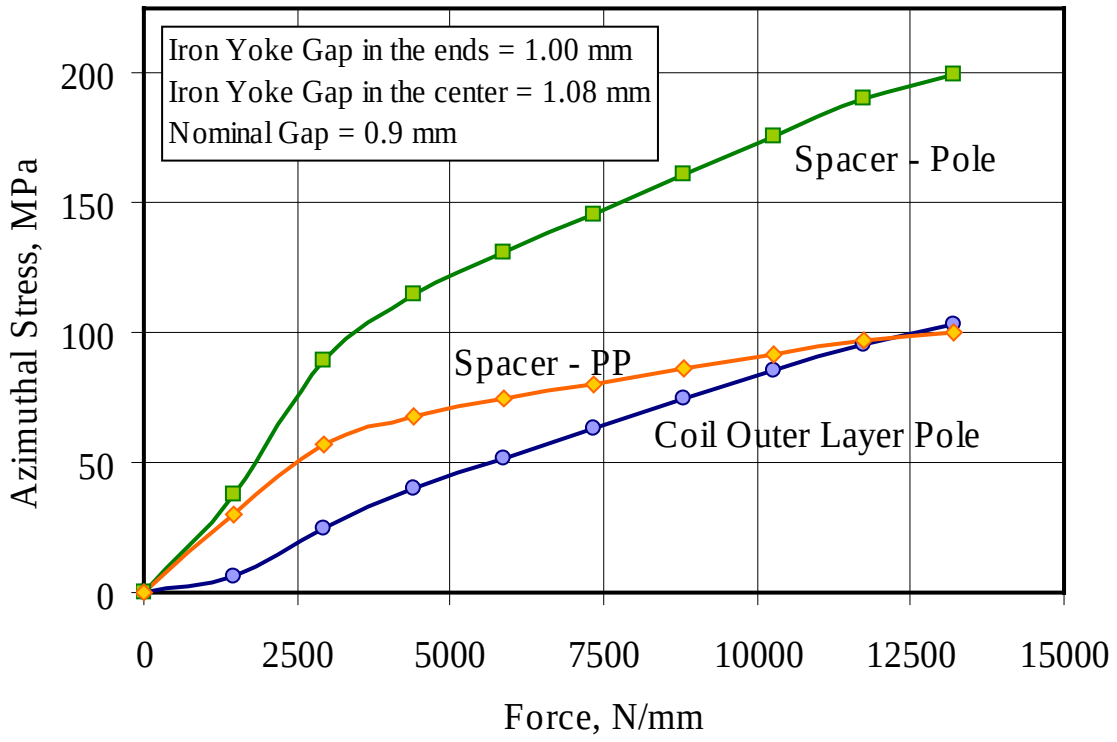

Figure 34: *Azimuthal stress variation during yoke assembly*.

8.0 Second Dipole Model

Coil size and reaction cycle needs to be optimized to eliminate the over sizing and tin leakage. Careful measurements are being taken to understand the geometry changes in the MJR Nb_3Sn cable during reaction with varying compaction pressures. With this data, the cable insulation scheme will be changed such that the coil azimuthal size will at nominal after reaction. To reduce the radial dimension, interlayer insulation will be reduced from three layers to two layers and the strip heaters will be moved to outer layer. The ground insulation will also be reduced by one layer. This will ensure that the coils will be assembled with little or no pressure in the reaction fixture. This along with the addition of low temperature heat-treatment step to the reaction cycle should eliminate the tin leakage.

Eventough the quality of impregnation was very good, we need to improve on the process such as better flow meter, hoses that can withstand 125 ^{o}C. The splice quality also needs to improved to prevent leaks. The curing temperature needs to be monitored such that it represents the coil temperature and not the oven temperature.